Smart Structures and Systems, *Vol. 30, No. 4 (2022) 421-432*
https://doi.org/10.12989/sss.2022.30.4.421

Novel integrative soft computing for daily pan evaporation modeling

Yu Zhang [1], LiLi Liu[*2a], Yongjun Zhu[**3b], Peng Wang [4] and Loke Kok Foong [5,6]

[1] *School of Geographic Sciencces and Tourism, Jiaying University, Meizhou 514015, Guangdong, China*
[2] *Ordos Water Conservancy Development Center, Ordos 017000, Inner Mongolia, China*
[3] *Paotai Soil Improvement Experimental Station, Shihezi 832000, Xinjiang, China*
[4] *College of Hydraulic and Civil Engineering, Xinjiang Agricultural University, Urumchi 830052, Xinjiang, China*
[5] *Institute of Research and Development, Duy Tan University, Da Nang, Vietnam*
[6] *School of Engineering & Technology, Duy Tan University, Da Nang, Vietnam*

(*Received October 12, 2020, Revised July 6, 2022, Accepted July 26, 2022*)

Abstract. Regarding the high significance of correct pan evaporation modeling, this study introduces two novel neuro-metaheuristic approaches to improve the accuracy of prediction for this parameter. Vortex search algorithms (VSA), sunflower optimization (SFO), and stochastic fractal search (SFS) are integrated with a multilayer perceptron neural network to create the VSA-MLPNN, SFO-MLPNN, and SFS-MLPNN hybrids. The climate data of Arcata-Eureka station (operated by the US environmental protection agency) belonging to the years 1986-1989 and the year 1990 are used for training and testing the models, respectively. Trying different configurations revealed that the best performance of the VSA, SFO, and SFS is obtained for the population size of 400, 300, and 100, respectively. The results were compared with a conventionally trained MLPNN to examine the effect of the metaheuristic algorithms. Overall, all four models presented a very reliable simulation. However, the SFS-MLPNN (mean absolute error, MAE = 0.0997 and Pearson correlation coefficient, R_P = 0.9957) was the most accurate model, followed by the VSA-MLPNN (MAE = 0.1058 and R_P = 0.9945), conventional MLPNN (MAE = 0.1062 and R_P = 0.9944), and SFO-MLPNN (MAE = 0.1305 and R_P = 0.9914). The findings indicated that employing the VSA and SFS results in improving the accuracy of the neural network in the prediction of pan evaporation. Hence, the suggested models are recommended for future practical applications.

Keywords: indirect measurement; neural network; pan evaporation; stochastic optimization algorithm

1. Introduction

Evaluation of pan evaporation (PE) has been of great importance, due to its effect on crucial subjects like hydrological research and climate change (Thom *et al*. 1981, Zuo *et al*. 2016). This climatic variable is widely regarded for decision making in agriculture, ecology, forestry, and hydrology e.g., proper water resource management and budget estimation (Shirsath and Singh 2010, Majhi and Naidu 2021). Up to now, many studies have introduced intelligent models, and more particularly artificial neural networks (ANNs), as capable predictive models for this parameter (Keskin and Terzi 2006, Ali Ghorbani *et al*. 2018, Mosavi *et al*. 2020, Zhao and Foong 2022). Such models, however, have been research hotspots in various fields of applications (Nehdi *et al*. 2006, Mohammadhassani *et al*. 2014, 2015, Shahbazi *et al*. 2014).

In a more comprehensive perspective, engineers have extensively benefited from the recent advances for facilitating complex simulations (Ahmadi *et al*. 2020, Zhao *et al*. 2022, Zhao and Wang 2022). This application comprises a wide range of domains from safety engineering (Chen *et al*. 2021) and material parameter analysis (Foong *et al*. 2021, Xie *et al*. 2021, Zhao *et al*. 2021) to hydrological estimations such as dew point temperature (Qasem *et al*. 2019, Zhang *et al*. 2022), wind speed (Band *et al*. 2022).

Kişi (2006) showed the efficiency of adaptive neuro-fuzzy inference system (ANFIS) for predicting the daily PE. For Daggett Station in California, the optimal configuration of ANFIS achieved a large coefficient of determination (R^2 = 0.998) which outperformed the ANN and Stephens–Stewart (SS) methods. Moreover, the values of mean absolute relative error obtained for the ANFIS were below the benchmark models. Genetic programming (GP) is another capable predictive tool that was used by Guven and Kişi (2011) for the same purpose. Majhi and Naidu (2020) employed a functional link ANN, as a less complex method than multi-layer ANN, for the daily PE modeling in agro-climatic areas of India. Referring to the root mean square errors (RMSEs) ranging in [0.85, 1.27] and [0.94, 1.58] for the functional link and multi-layer ANN, respectively, it was demonstrated that the proposed model provides a more efficient prediction. Likewise, Malik *et al*. (2020) demonstrated the high applicability of multiple model ANN for simulating the monthly PE in India. The potential of two popular ANNs, namely radial basis function (RBF) and multilayer perceptron (MLP), as well as support vector

*Corresponding author,
E-mail: whmliulili@126.com
**Co-corresponding author,
E-mail: wandd2010@126.com

ISSN: 1738-1584 (Print), 1738-1991 (Online)

regression (SVR), was demonstrated by Tezel and Buyukyildiz (2016). The feasibility of further intelligent approaches applied to evaporation issues has been studied in the literature (extreme learning machine (Sebbar *et al*. 2019), the ANFIS with different learning strategies (Adnan *et al*. 2019), random forest (Singh *et al*. 2020), Gaussian process regression (Shabani *et al*. 2020), etc.).

Many researchers have attempted to denote the most capable models through conducting comparative studies. In a study by Wang *et al*. (2017), for example, the performance of eight models consisting of six commonly used intelligent tools (MLPNN, fuzzy genetic (FG), generalized regression neural network (GRNN), least-square support vector machine (LSSVM), grid partition ANFIS (ANFIS-GP), and multivariate adaptive regression spline (MARS)) and two regression-based approaches (the SS and multiple linear regression (MLR)) was evaluated for the PE estimation. In addition to the suitability of the used models, they professed the higher ability of the ANN-based models. Eray *et al*. (2018) compared the competency of dynamic evolving neural-fuzzy inference system (DENFIS) and multi-gene GP for the PE modeling in the Mediterranean areas of Turkey. While the classical GP was the superior model for analyzing the date of Antakya station, the DENFIS presented the most reliable prediction for Antalya station. Further comparitive studies among machine learning tools are available in Ref.s (Wang *et al*. 2016, Nourani *et al*. 2019, Sebbar *et al*. 2020, Shiri *et al*. 2020).

Moreover, various engineering parameters (e.g., rainfall pattern (Yaseen *et al*. 2018), slope stability (Luat *et al*. 2020), solar radiation (Rezaie-Balf *et al*. 2019), dew point temperature (Naganna *et al*. 2019), river streamflow (Mohammadi *et al*. 2020), rainfall-runoff (Roy *et al*. 2019), beam shear capacity (Nehdi and Greenough 2007), etc.) have been successfully modeled using stochastic optimization techniques (Nguyen *et al*. 2019). Wu *et al*. (2020) combined the extreme learning machine (ELM) model flower pollination algorithm and whale optimization algorithm (WOA) to predict the PE. They observed that these two hybrid models not only present a reliable prediction of this parameter but also perform more accurately than classical models like ANN and M5 model tree. A bat algorithm-optimized XGBoost was suggested by Han *et al*. (2019) as a reliable tool for estimating reference evapotranspiration. Ashrafzadeh *et al*. (2018) built a hybrid model by synthesizing firefly algorithm (FA) with ANN. They applied the proposed model to two weather stations in Iran. It was shown that, compared to the typical ANN, the hybrid model provides a more reliable estimation of the PE (the RMSEs of 1.088 vs. 0.871 at Anzali station and 1.197 vs. 0.855 at Astara station). The same methodology was used by Ghorbani *et al*. (2018) for Manjil and Talesh stations, northern Iran. The feasibility of three metaheuristic algorithms, namely genetic algorithm (GA), grey wolf optimization (GWO), and the WOA coupled with ANN was investigated by Seifi and Soroush (2020). The models were applied to five different areas of Iran and it was shown that the GA creates a more powerful ANN for Astara, Gorgan, and Tabas stations (with the R^2s of 0.83, 0.79, and 0.86, respectively). Wang *et al*. (2020) used a combination of kernel-based nonlinear Arps decline (KNEA) and salp swarm algorithm (SSA) for the PE simulation in arid and semi-arid areas in China. They concluded the overall superiority of the proposed model over traditional intelligent models. Ashrafzadeh *et al*. (2019) trained the MLP using the KH algorithm. The use of this algorithm resulted in reducing the RMSE from 1.088 to 0.725 in station 1 and from 1.197 to 0.855 in station 2. Both models, however, outperformed the SVM.

Other machine learning models like SVR have shown high potential in combination with metaheuristic techniques (e.g., the FA (Moazenzadeh *et al*. 2018), WOA (Mohammadi and Mehdizadeh 2020), and krill herd (KH) algorithm (Guan *et al*. 2020)). In similar efforts, scholars like Mohamadi *et al*. (2020) and Khosravi *et al*. (2019) have examined the applicability of ANFIS optimized by techniques like the FA and shark algorithm, GA, imperialistic competitive algorithm, etc.

All in all, the literature review introduces metaheuristic algorithms as suitable ways toward improving the accuracy of soft computing approaches (Moayedi *et al*. 2021, Yang *et al*. 2021). Hence, this study is dedicated to employ three novel types of these algorithms, namely vortex search algorithms (VSA), sunflower optimization (SFO), and stochastic fractal search (SFS) for creating optimal hybrids

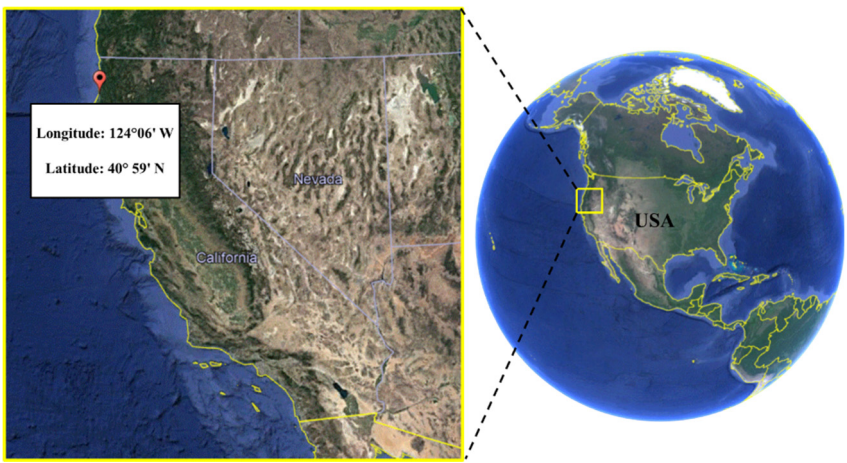

Fig. 1 Location of the Arcata-Eureka station

of neural network in predicting the PE. To the best knowledge of the authors, these algorithms are among the new generation of metaheuristic family and have not been previously used for the same objective. Hence, their application in this work would open the door for other and newer metaheuristic algorithms to contribute to solving similar environmental issues. The results of the proposed models are compared with the classical ANN to address their effectiveness. The efficiency of the VSA, SFO, and SFS is also compared to point out the most suitable optimizer.

2. Methodology and data

2.1 Study area

The climate data for analyzing and predicting the daily PE are provided by an automated weather station that is operated by the US environmental protection agency (EPA, website: http://www.epa.gov). The name of the purposed station is Arcata-Eureka (station WBAN number: 24283). Fig. 1 shows that this station is located in a coastal region, North-West of California. Note that this case has been studied by Kişi (2006) using simple predictive models.

In addition to the PE as the target parameter, the daily records of solar radiation (SR), temperature (T), wind speed (WS), humidity (H), and pressure (P) are taken as the PE influential factors. According to the EPA website, the data are available up to the year 1991. The records belonging to the latest five-years were downloaded for this study. Fig. 2 illustrates the time-series of the obtained dataset.

Based on the ratio of 80:20, the data of the first four years (from January 01, 1986 to December 31, 1989) is considered as the training group. This group is used to analyze the non-linear dependence of the PE on T, WS, SR, P, and H. Once the models learned the desired pattern, they perform to predict the PE for the days from January 01, 1990 to December 31, 1990. This group is called testing dataset. Table 1 describes the training and testing datasets by giving average, skewness, sample variance, standard deviation, minimum, and maximum values. According to this table, the air temperature was below 18.9°C over the intended period. Also, it demonstrates that the PE ranged between 0.1 and 7.8 *mm*/*day*.

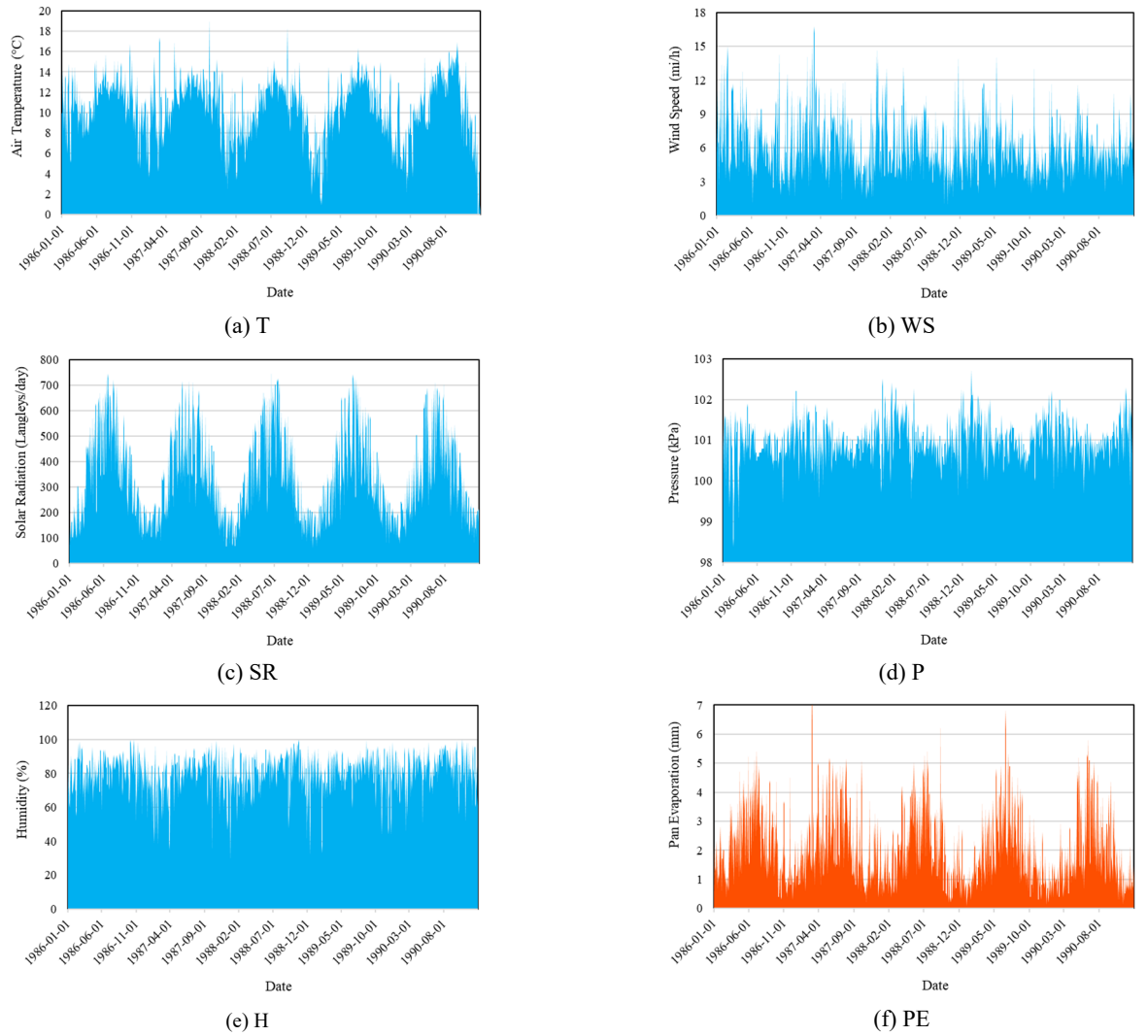

(a) T (b) WS

(c) SR (d) P

(e) H (f) PE

Fig. 2 Graphical time-series of the PE and input factors

Table 1 Descriptive statistics of the used datasets

Phase	Parameter	Indicator					
		Average	Skewness	Sample variance	Standard deviation	Minimum	Maximum
Testing	**T** (°*C*)	10.2	-0.7	14.3	3.8	-4.2	16.9
	WS (*mi*/*h*)	5.9	0.9	3.8	1.9	1.8	15.7
	SR (*Langley*)	338.2	0.6	29182.6	170.8	62.4	751.0
	P (*Kpa*)	101.1	0.0	0.2	0.5	99.5	102.3
	H (%)	82.5	-0.8	105.5	10.3	46.0	100.0
	PE (*mm*)	1.9	1.1	1.6	1.3	0.1	6.4
Training	**T** (°*C*)	10.6	-0.6	7.4	2.7	0.4	18.9
	WS (*mi*/*h*)	6.1	0.8	7.3	2.7	0.6	18.6
	SR (*Langley*)	336.1	0.5	30308.1	174.1	54.6	749.6
	P (*Kpa*)	101.0	-0.1	0.3	0.5	98.4	102.7
	H (%)	80.4	-1.3	124.9	11.2	27.0	100.0
	PE (*mm*)	2.1	0.8	1.6	1.3	0.1	7.8

2.2 Methodology

2.2.1 The VSA algorithm

The name VSA represents a recently-developed metaheuristic method that mimics the structure of natural vortices. This algorithm was designed by Doğan and Ölmez (2015). During the optimization process, the algorithm deals with two major steps dedicated to finding local and global best solutions. A significant factor that affects the quality of the solution is the fitness of the surrounding particles.

In the beginning, a number of circles seek the solution within the created space. The initial center point (μ_0) and a primary radius should be determined. Given UL and LL as the upper and lower limit of the defined problem, Eq. (1) determines the μ_0

$$\mu_0 = \frac{UL + LL}{2} \tag{1}$$

In the VSA, a Gaussian distribution in an S-dimensional space is used to generate the candidate solutions as shown in Eq. (2).

$$p(y\,|\mu,\Sigma) = \frac{1}{\sqrt{(2\pi)^S|\sum|}} exp\left\{\frac{-1}{2}(y-\mu)^T\sum^{-1}(y-\mu)\right\} \tag{2}$$

where y is the vector of the random variable, $\sum$ stands for the covariance matrix, and T is the transposition indicator. The distribution will take a spherical shape, once all of the diagonal variances of Σ are the same and there is an uncorrelated covariance as follows

$$\Sigma = \sigma^2.\mathrm{I}_{S\times S} \tag{3}$$

in which, σ^2 symbolizes the spherical distribution variance and $\mathrm{I}_{S\times S}$ is the identity matrix. The diameter of the initial circle is calculated using Eq. (4).

$$\sigma_0 = \frac{max\,(UL) - min\,(LL)}{2} \tag{4}$$

As is seen, this equation finds the radius using the maximum and minimum values of the UL and LL. However, since some solutions may exceed these boundaries, Eq. (5) is used to shift the violating solutions into the limitations

$$sol_i^k = rand\,.(UL^i - LL^i) + LL^i \tag{5}$$

where k and i give the number of solutions and the dimension value, respectively. Also, $rand$ is a random variable for providing the random distribution of the intended solution.

The found solution is regularly compared with that of the previous iteration. The algorithm saves the optimal solution based on the below relationship

$$Error\,(Solution\,i) < Error\,(Optimal\,solution),\quad Optimal\,solution = Solution\,i \tag{6}$$

In the following, the center of the circle is placed where the optimal solution is acquired in the earlier iteration. The algorithm, simultaneously, reduces the radius of the circle to search only the areas wherein the best optimal solution can be found. This reduction process can be expressed as follows

$$r_t = \sigma_0\left(\frac{1}{x}\right) gammaincv\,(x, m_t), \quad m_t = m_0 - \frac{t}{T} \tag{7}$$

where $gammaincv$ represents the inverse of the Gamma function, T is the maximum number of iterations, and the coefficient m_t is used for adjusting the search vector resolution (Altintasi *et al*. 2020).

2.2.2 The SFO algorithm

Inspired by the act of sunflowers in following the sunlight as well as their pollination behavior, Gomes *et al*.

(2019) introduced the SFO as a new metaheuristic algorithm. The inverse square law radiation is also considered in this algorithm. Based on Eq. (8), the R_S intensity (IR_S) decreases with the increase in the distance between the sun and flower.

$$IR_S = \frac{P_S}{4\pi r^2} \tag{8}$$

where r gives the distance between the sun and flower and P_S represents the sun's power.

Given X_i and X_{best} as the current and the best position of the flowers, respectively, Eq. (9) expresses the direction of plants towards the sun.

$$\overrightarrow{S_i} = \frac{X_{best} - X_i}{\|X_{best} - X_i\|} \tag{9}$$

The following equation gives the step of the flowers in the sun direction

$$d_i = \beta \times P_i\left(\|X_i + X_{i-1}\|\right) \times \|X_i + X_{i-1}\| \tag{10}$$

In the above relationship, inertial displacement of the flowers is represented by β and $P_i\left(\|X_i + X_{i-1}\|\right)$ gives the pollination probability wherein the i^{th} flower fertilizes the i-1^{th} to generate new individuals. Eq. (10) calculates the maximum step.

$$d_{max} = \frac{\|X_{max} - X_{min}\|}{2 \times N_p} \tag{11}$$

in which N_p stands for the number of flowers, and X_{min} and X_{max} are lower and higher constraints.

In the SFO, updating the positions is carried out using the below equation (Qais *et al*. 2019)

$$\overrightarrow{X_{i+1}} = \overrightarrow{X_i} + d_i \times \overrightarrow{S_i} \tag{12}$$

Further explanations about the SFO can be found in studies like (Shaheen *et al*. 2019, Alshammari and Guesmi 2020).

2.2.3 The SFS algorithm

Salimi (2015) introduced the SFS as a capable optimizer in 2015. This technique uses fractal properties to optimize different problems. Two major operations in the SFS are named diffusion and update processes. In the first operation, the search space is exploited by the points that diffuse around their current position. This action reduces the danger of local minima. Through a Gaussian walk, new ponits are generated based on the below equations

$$X_{i,new1} = G\left(\mu_{X_{best}}, \sigma\right) + (\tau \times X_{best} - \tau' \times X_i) \tag{13}$$

$$X_{i,new2} = G(\mu_X, \sigma) \tag{14}$$

in which $\mu_{X_{best}} = X_{best}$ and $\mu_X = X_i$. Also, σ is obtained based on Eq. (15).

$$\sigma = \left|\frac{\log(It)}{It}\left(X_i - X_{best}\right)\right| \tag{15}$$

where $\frac{\log(t)}{t}$ is applied for improving the local search ability through reducing the Gaussian jump size over the iteration It.

In the next operation (i.e., updating process), the algorithm uses two statistical procedures for implementing an efficient search in the problem space. It first ranks the points with respect to their fitness. Next, each point receives a probability value that is calculated as follows

$$PV_i = \frac{\text{rank}\,(X_i)}{N_P} \tag{16}$$

According to Eq. (16), the higher values of the PV indicate better points. Eq. (17) is applied to update the j^{th} component of the point i.

$$\begin{matrix} X_i'(j) = X_r(j) - \tau \times \left(X_t(j) - X_i(j)\right) & \text{if } PV < \tau \\ X_i'(j) = X_i(j) & \text{otherwise} \end{matrix} \tag{17}$$

The algorithm ranks the new points (i.e., X_i's) to implement the second procedure. Again, the new PV (PV') is considered for the updating process. Once $PV' < \tau'$, the algorithm updates the position of the X_i' by Eq. (18). Otherwise, it remains unchanged (Tran *et al*. 2020).

$$\begin{cases} X_i'' = X_i' - \tau' \times (X_t' - X_{best}) & if\ \tau' \le 0.5 \\ X'' = X_i' + \tau' \times (X_t' - X_r') & if\ \tau' > 0.5 \end{cases} \tag{18}$$

More information about the SFS can be found in (Mosbah and El-Hawary 2017, Çelik 2020).

2.3 Accuracy indicators

Mean absolute error (MAE), RMSE, and mean absolute percentage error (MAPE) are three error indicators that along with Pearson correlation coefficient (R_P) report the accuracy of prediction for the used models. Given $PE_{i_{prediction}}$ and $PE_{i_{reality}}$ as the modeled and measured PEs, as well as S as the number of compared PE pairs, Eqs. (19) to (22) express the formulization of the MAE, RMSE, MAPE, and R_P, respectively.

$$MAE = \frac{1}{S}\sum_{i=1}^{S}\left|PE_{i_{reality}} - PE_{i_{prediction}}\right| \tag{19}$$

$$RMSE = \sqrt{\frac{1}{S}\sum_{i=1}^{S}\left[\left(PE_{i_{reality}} - PE_{i_{prediction}}\right)\right]^2} \tag{20}$$

$$MAPE = \frac{1}{S}\sum_{i=1}^{S}\left|\frac{PE_{i_{reality}} - PE_{i_{prediction}}}{PE_{i_{reality}}}\right| \times 100 \tag{21}$$

$$R_P = \frac{\sum_{i=1}^{S}(PE_{i_{prediction}} - \overline{PE}_{prediction})(PE_{i_{reality}} - \overline{PE}_{reality})}{\sqrt{\sum_{i=1}^{S}(PE_{i_{prediction}} - \overline{PE}_{prediction})^2}\sqrt{\sum_{i=1}^{S}(PE_{i_{reality}} - \overline{PE}_{reality})^2}} \quad (22)$$

3. Results and discussion

3.1 Optimization and training

It was earlier explained that, in this work, the duty of training the MLP neural network is appointed to the VSA, SFO, and SFS metaheuristic algorithms. By combining these networks, three hybrids of VSA-MLPNN, SFO-MLPNN, and SFS-MLPNN were created. The conventional MLPNN (CMLPNN) that is supervised by Levenberg–Marquardt (LM) algorithm (Moré 1978), is also implemented as a benchmark.

To implement the hybrid models, below steps were followed:

a) A 5×4×1 MLPNN was selected based on a trial-and-error effort
b) The formulation of the MLPNN was given to each algorithm to have a combined model
c) A large number of iterations is required to ensure that the algorithms reach a desirable optimal response. Based on the optimization proceedings, all three algorithms were implemented with 1000 iterations.
d) The effect of the number of search agents (i.e., the population size, N_{SW}) was examined for each algorithm to employ an appropriate population.

Figs. 3(a), (b), and (c) show the convergence curves obtained after executing six N_{SW}s for the VSA-MLPNN, SFO-MLPNN, and SFS-MLPNN, respectively. As is seen, although the curves of the algorithms pass through different ways in the beginning, they reach a very close objective function at the end. This is worth noting that the RMSE of the training PEs reflected the objective function in each iteration. Hence, the latest values of the objective function represent the training RMSE.

Fig. 3 indicates that the best training of the MLPNN is achieved by the VSA, SFO, and SFS implemented with the N_{SW}s of 400, 300, and 100, respectively. While the training RMSE of the VSA-MLPNN (0.1521) and SFO-MLPNN (0.2060) are above the CMLPNN (0.1464), applying the SFS diminished this error to 0.1351. Moreover, based on the respective MAPEs of 6.7963, 7.0966, 9.7227, and 6.4018%, and the MAEs of 0.0999, 0.1027, 0.1367, and 0.0919 for the CMLPNN, VSA-MLPNN, SFO-MLPNN, and SFS-MLPNN, it is deduced that the SFS captures the most profound understanding of the PE behavior. This excellence can also be professed by the R_Ps of 0.9933, 0.9928, 0.9868, and 0.9943.

Regarding the time of optimization, implementing the VSA, SFO, and SFS (i.e., with the NSWs of 400, 300, and 100), took around 3624, 3898, and 6085 seconds, respectively. Noting that the used computer was a 64-bit system with Intel Core i7 @ 1.80 GHz and 16 gigs of RAM.

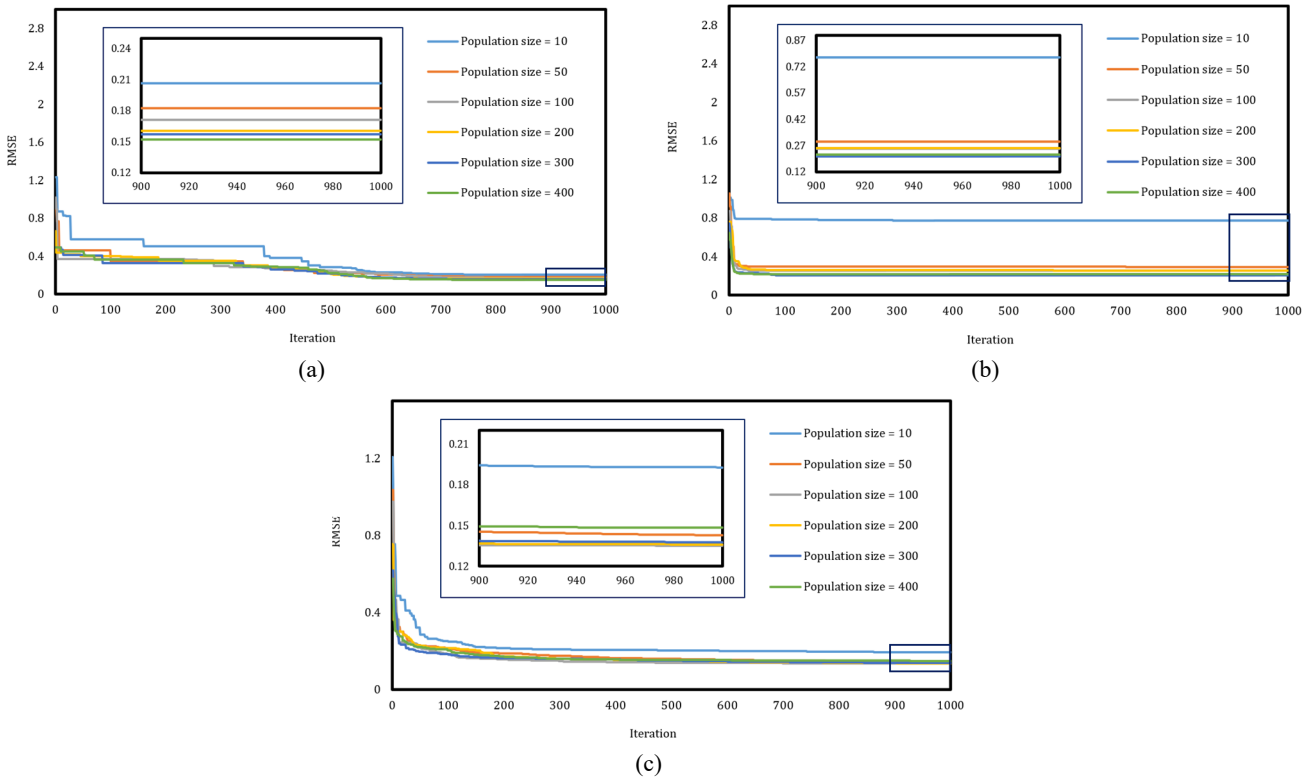

Fig. 3 The convergence proceeding of (a) VSA-MLPNN, (b) SFO-MLPNN, and (c) SFS-MLPNN hybrids

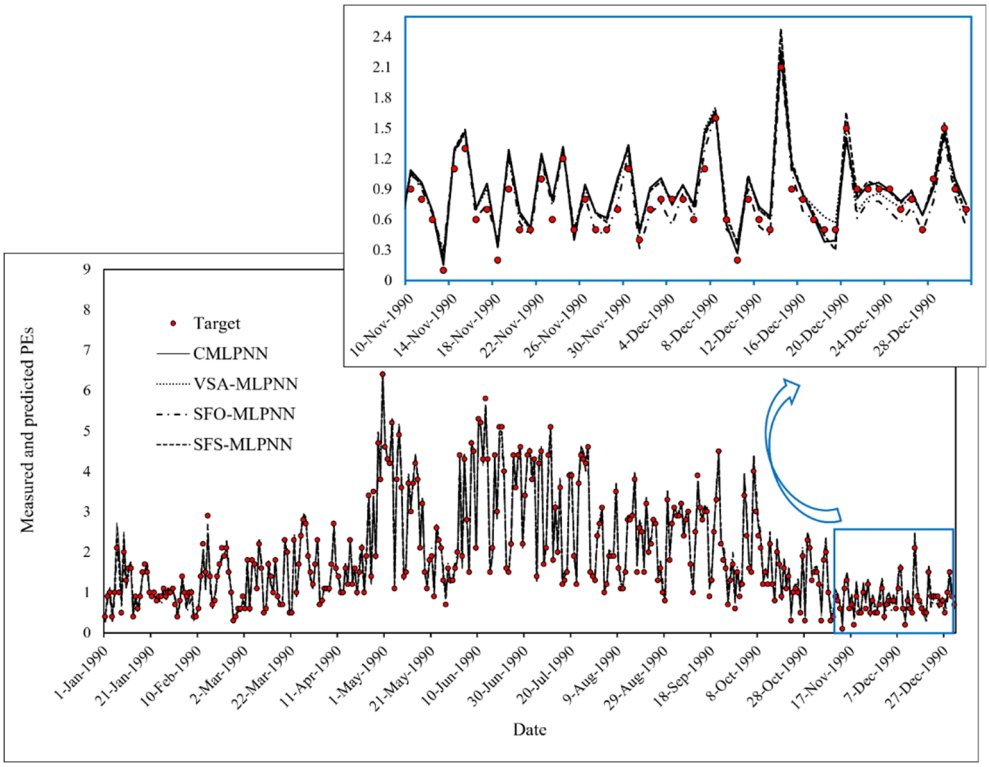

Fig. 4 Comparison between the modeled and measured PEs for the testing period

The SFS, despite being the most powerful algorithm, demands considerably higher time for optimizing the MLPNN. Likewise, the VSA was slightly faster than SFO.

3.2 Prediction of the PE

The trained CMLPNN, VSA-MLPNN, SFO-MLPNN, and SFS-MLPNN then predicted the PE for the year 1990 as an indication of new input values (i.e., T, WS, SR, P, and H). Therefore, the quality of prediction in the test phase reflects the reliability of the models in dealing with future climate conditions.

The PEs predicted by each intelligent model were compared with the measured values to denote the corresponding level of accuracy. Fig. 4 does this comparison graphically. As is seen, the PE changes have been correctly followed by all used models. For example, the smallest PE is 0.1 *mm* (measured on November 13, where the daily T, WS, SR, P, and H were 10.1°*C*, 5.2 *mi*/*h*, 71.7 *Langley*, 100.7 *Kpa*, and 99%, respectively) that is predicted as 0.1568, 0.2413, 0.2924, and 0.2261 *mm* by the CMLPNN, VSA-MLPNN, SFO-MLPNN, and SFS-MLPNN, respectively. As for the largest PE, it is 6.4 *mm* (measured on April 30, where the daily T, WS, SR, P, and H were 12.0°*C*, 11.5 *mi*/*h*, 651.8 *Langley*, 101.1 *Kpa*, and 48%) that is predicted as 6.1695, 6.3801, 6.4233, and 6.4243 *mm*.

In this phase, all error indicators obtained for the CMLPNN (the RMSE, MAPE, and MAE of 0.1436, 8.8273%, and 0.1062) were smaller than those of the SFO-MLPNN (0.1699, 11.3010%, and 0.1305). The RMSE of the CMLPNN was degraded to 0.1398 and 0.1289 after letting the VSA and SFS capture the PE pattern. Likewise, its MAE fell to 0.1058 by the VSA, and more tangibly, to 0.0997 by the SFS optimizer. But, unlike these indicators, the MAPE was reduced by only the SFS (= 8.5787%). In this relation, the MAPE of the VSA-MLPNN was 9.4047% which is slightly higher than the CMLPNN.

Figs. 5(a), (c), (e), and (g) show the frequency (i.e., the histogram) of the errors in the testing phase. Here, the difference between the $PE_{i_{prediction}}$ and $PE_{i_{reality}}$ for the i^{th} day is referred to as Error. Moreover, the regression charts of the corresponding predictions are depicted in Figs. 5(b), (d), (f), and (h). As is seen, both factors (i.e., the frequency of the errors and the consistency of the results) indicate an excellent level of accuracy for all used models. By comparison, however, the R_Ps obtained for the SFS-MLPNN and VSA-MLPNN are larger than CMLPNN (0.9957 and 0.9945 vs. 0.9944). Also, the poorest correlation is observed for the products of the SFO-MLPNN (R_P = 0.9914).

3.3 Comparison

Two earlier sections reported that replacing the regular training strategy of the MLPNN (i.e., the LM algorithm) with the SFS results in a stronger evaluative model. More specifically, this metaheuristic scheme surpassed the LM in tuning the biases and weights of the neural network. It was demonstrated by all four accuracy indicators in the training phase. Another conclusion from this assessment is the higher searching potential of the VSA in comparison with the SFO.

Due to the same reason, in the testing phase, the MLPNN constructed by the response of the SFS enjoys more accuracy of prediction for stranger environmental

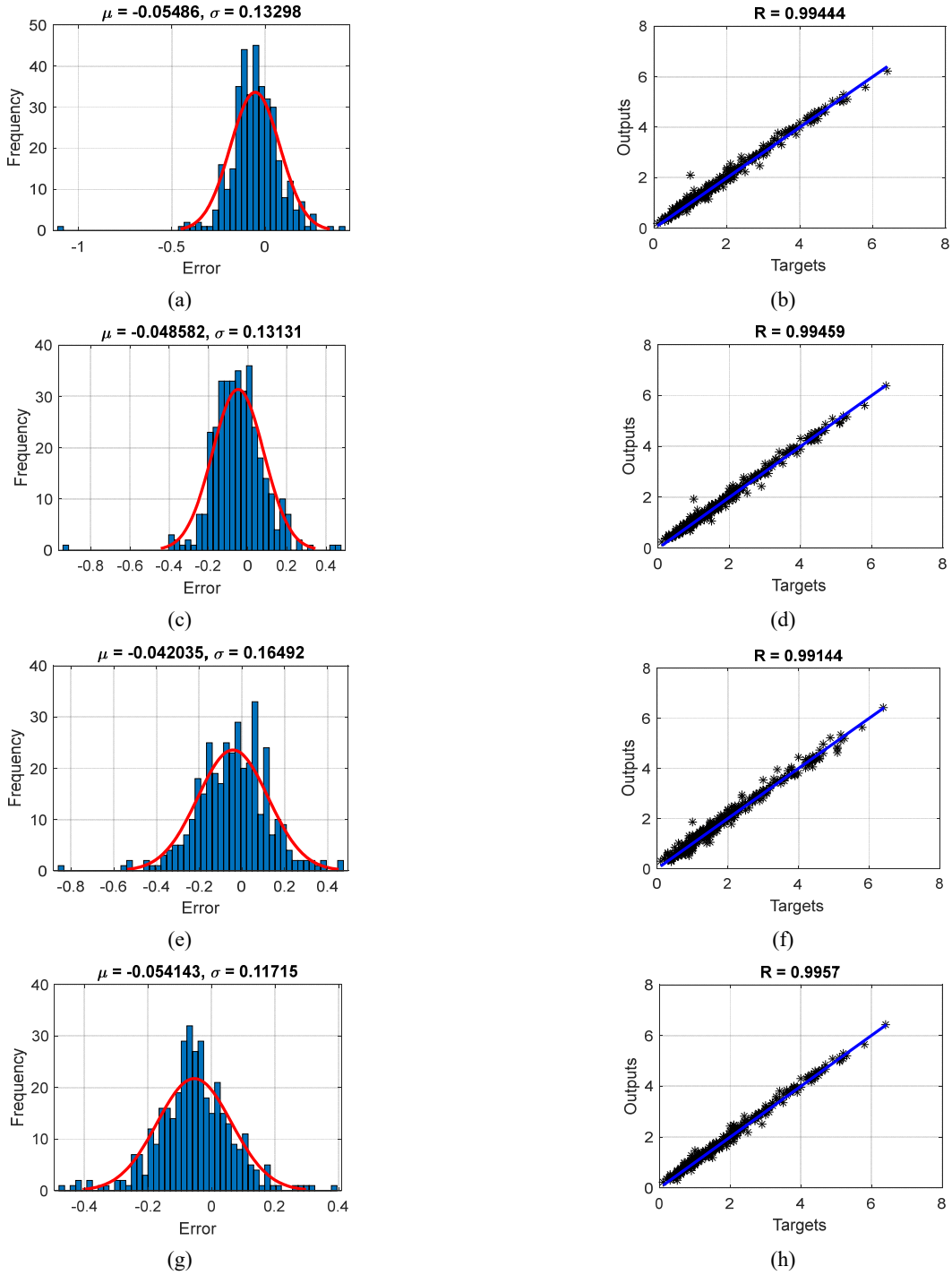

Fig. 5 Histogram of the errors and regression charts of the testing samples for the estimation of (a) and (b) CMLPNN; (c) and (d) VSA-MLPNN; (e) and (f) SFO-MLPNN; and (g) and (h) SFS-MLPNN (where μ: Mean error, σ: Standard error, and R: Pearson correlation coefficient)

circumstances. Accordingly, higher generalizability can be deduced for the network parameters suggested by this algorithm. However, the excellent robustness of the VSA should not be ignored as well.

3.4 Formula extraction

When an MLPNN aims to predict a parameter, the calculations are as follows: (a) receiving the input parameters in the input layer, (b) in the middle layer, multiplying the inputs to specific weights and summing them with bias, (c) applying an activation function to the whole, (d) using the outcome for similar calculations in the subsequent layers (here, output layer).

Referring to the superiority of the SFS, it is aimed to build a predictive formula from the SFS-MLPNN model. Considering the architecture of the basic neural network (i.e., a 5×4×1 MLP), the solution discovered by the used

trainers consists of five biases (four for the hidden layer and one for the output layer) plus 24 weights (20 input-hidden weights and 4 hidden-output weights). This section shows how these parameters are organized in an MLPNN.

Moving along the network, the input factors (i.e., T, WS, SR, P, and H) received by the neurons of the first layer are processed in the four hidden neurons as follows

$$\begin{bmatrix} O_{HN1} \\ O_{HN2} \\ O_{HN3} \\ O_{HN4} \end{bmatrix} = Tansig\left(\left(\begin{bmatrix} 1.210265 & -0.952152 & -0.070341 & 0.622368 & -0.805564 \\ 1.156421 & -0.726730 & 1.145546 & -0.483049 & -0.038713 \\ -1.075352 & -0.303202 & 1.027936 & -0.485886 & 0.933546 \\ -0.982187 & -1.077283 & 0.672922 & 0.022296 & -0.913241 \end{bmatrix}\begin{bmatrix} T \\ WS \\ SR \\ P \\ H \end{bmatrix}\right) + \begin{bmatrix} -1.847311 \\ -0.615770 \\ -0.615770 \\ -1.847311 \end{bmatrix}\right) \quad (23)$$

where O_{HN1}, O_{HN2}, O_{HN3}, and O_{HN4} represent the outputs of the hidden neurons and $\text{Tansig} = \frac{2}{1+e^{-2x}} - 1$ is the activation function. Next, the output neuron performs the following calculations to release the PE.

$$PE_{SFS-MLPNN} = -0.731480 \times O_{HN1} - 0.068773 \times O_{HN2} + 0.086183 \times O_{HN3} + 0.793489 \times O_{HN4} + 0.016297 \quad (24)$$

These variables were directly extracted from the trained network of the SFS-MLPNN using the command "getwb ()" and they were then organized using "separatewb ()" in the MATLAB environment.

3.5 Further discussion

In this work, different solutions were provided based on metaheuristic science for a crucial hydrological issue, namely predicting the pan evaporation. These models have also previously served widely for other environmental issues (Mehrabi *et al.* 2020, Moayedi *et al.* 2020, Mehrabi and Moayedi 2021). The accuracy of the models was sufficient to be practically used for new cases. However, as a limitation, testing the models with further external data (e.g., other stations) would further confirm the generalizability of the solutions. It is a good subject for future works because in this work the main objective was introducing novel methodology.

The simulation done used a non-linear dataset in which the PE was treated as a function of several environmental factors. The correlation index (R^2) between the PE and T, WS, SR, P, and H was 0.1881, 0.1462, 0.7228, 0.0204, and 0.1921, respectively. These values indicate that the SR is the most correlated parameter with PE. Moreover, an unbiased importance assessment is performed to further evaluate the role of input data in determining the value of PE. This evaluation relies on a random forest model that investigates the effects by permuting the data (Zheng *et al.* 2020, Mehrabi 2021). The results are shown in Fig. 6. According to these results, SR is the most contributive factor, followed by H, WS, and T, and P has the smallest contribution. These results are in agreement with correlation analysis. Hence, for practical applications the factor P can be disregarded in order to make a less complex network.

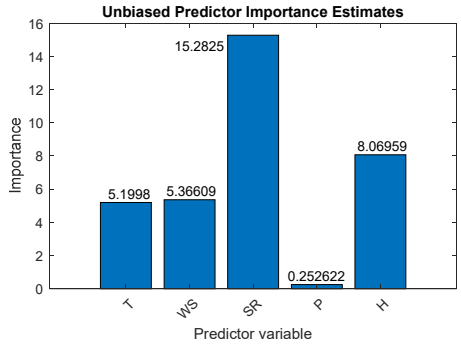

Fig. 6 Importance assessment of the inputs

An explicit formula was also extracted which can be directly used for predicting the PE without the need of using any programming language or GUI (Seyedashraf *et al.* 2018). As a limitation of the formula, it is applicable only for places where the selected input factors are available for it.

A sensitivity analysis was required for determining the best population size of each algorithm (Moayedi *et al.* 2019a, b). However, in some cases, a very close performance was observed for the algorithm which, if it is generally a powerful algorithm, it can be an advantage because lower populations usually yield faster solutions.

4. Conclusions

The artificial neural network has been a leading tool for different hydrological modelings. But many earlier studies have shown the competency of metaheuristic techniques in optimizing them. Three novel strategies of vortex search algorithms, sunflower optimization, and stochastic fractal search were coupled with an MLPNN to predict the pan evaporation. In summary, the findings professed an excellent capability of learning and reproducing the PE behavior for the used models. Since the elite configuration of SFS-based hybrid outperformed the conventionally trained MLPNN in capturing the PE pattern, it was deduced that the SFS is a stronger algorithm compared to the Levenberg-Marquardt. In the testing phase, the decline of the RMSE and MAE, as well as the increase of the R_P, indicated the better performance of the VSA-MLPNN and SFS-MLPNN. Therefore, the proposed models can be considered as reliable predictive tools for real-world projects. The last part of the work was dedicated to presenting an explicit formulation of the most successful model (i.e., the SFS-MLPNN) as a PE predictive formula.

Funding

This work was supported by Science and Technology Program of Guangdong Province (2020B121201013); Natural Science Foundation of Guangdong Province (2021A1515012597); Rural Science and Technology Commissioner Program of Guangdong Province (KTP20200278); Inner Mongolia Science and Technology Innovation Guide project (Integration and demonstration of planting quinoa quad-winged in Ordos).

References

Adnan, R.M., Malik, A., Kumar, A., Parmar, K.S. and Kisi, O. (2019), "Pan evaporation modeling by three different neuro-fuzzy intelligent systems using climatic inputs", *Arab. J. Geosci*., **12**(20), 606. https://doi.org/10.1007/s12517-019-4781-6

Ahmadi, M.H., Baghban, A., Sadeghzadeh, M., Zamen, M., Mosavi, A., Shamshirband, S., Kumar, R. and Mohammadi-Khanaposhtani, M. (2020), "Evaluation of electrical efficiency of photovoltaic thermal solar collector", *Eng. Applicat. Computat. Fluid Mech*., **14**(1), 545-565. https://doi.org/10.1080/19942060.2020.1734094

Ali Ghorbani, M., Kazempour, R., Chau, K.W., Shamshirband, S. and Taherei Ghazvinei, P. (2018), "Forecasting pan evaporation with an integrated artificial neural network quantum-behaved particle swarm optimization model: a case study in Talesh, Northern Iran", *Eng. Applicat. Computat. Fluid Mech*., **12**(1), 724-737. https://doi.org/10.1080/19942060.2018.1517052

Alshammari, B.M. and Guesmi, T. (2020), "New chaotic sunflower optimization algorithm for optimal tuning of power system stabilizers", *J. Electr. Eng. Technol*., 1-13. https://doi.org/10.1007/s42835-020-00470-1

Altintasi, C., Aydin, O., Taplamacioglu, M.C. and Salor, O. (2020), "Power system harmonic and interharmonic estimation using Vortex Search Algorithm", *Electric Power Syst. Res*., **182**, 106187. https://doi.org/10.1016/j.epsr.2019.106187

Ashrafzadeh, A., Malik, A., Jothiprakash, V., Ghorbani, M.A. and Biazar, S.M. (2018), "Estimation of daily pan evaporation using neural networks and meta-heuristic approaches", *ISH J. Hydraulic Eng*., **26**(4), 421-429. https://doi.org/10.1080/09715010.2018.1498754

Ashrafzadeh, A., Ghorbani, M.A., Biazar, S.M. and Yaseen, Z.M. (2019), "Evaporation process modelling over northern Iran: application of an integrative data-intelligence model with the krill herd optimization algorithm", *Hydrol. Sci. J*., **64**(15), 1843-1856. https://doi.org/10.1080/02626667.2019.1676428

Band, S.S., Ardabili, S., Mosavi, A., Jun, C., Khoshkam, H. and Moslehpour, M. (2022), "Feasibility of soft computing techniques for estimating the long-term mean monthly wind speed", *Energy Reports*, **8**, 638-648. https://doi.org/10.1016/j.egyr.2021.11.247

Çelik, E. (2020), "Improved stochastic fractal search algorithm and modified cost function for automatic generation control of interconnected electric power systems", *Eng. Applicat. Artif. Intell*., **88**, 103407. https://doi.org/10.1016/j.engappai.2019.103407

Chen, Y., Lin, H., Cao, R. and Zhang, C. (2021), "Slope stability analysis considering different contributions of shear strength parameters", *Int. J. Geomech*., **21**(3), 04020265. https://doi.org/10.1061/(ASCE)GM.1943-5622.0001937

Doğan, B. and Ölmez, T. (2015), "A new metaheuristic for numerical function optimization: Vortex Search algorithm", *Information Sciences*, **293**, 125-145. https://doi.org/10.1016/j.ins.2014.08.053

Eray, O., Mert, C. and Kisi, O. (2018), "Comparison of multi-gene genetic programming and dynamic evolving neural-fuzzy inference system in modeling pan evaporation", Hydrology Research, **49**(4), 1221-1233. https://doi.org/10.2166/nh.2017.076

Foong, L.K., Zhao, Y., Bai, C. and Xu, C. (2021), "Efficient metaheuristic-retrofitted techniques for concrete slump simulation", *Smart Struct. Syst*., *Int. J*., **27**(5), 745-759. https://doi.org/10.12989/SSS.2021.27.5.745

Ghorbani, M.A., Deo, R.C., Yaseen, Z.M., H Kashani, M. and Mohammadi, B. (2018), "Pan evaporation prediction using a hybrid multilayer perceptron-firefly algorithm (MLP-FFA) model: case study in North Iran", Theoretical and applied climatology, **133**(3-4), 1119-1131. https://doi.org/10.1007/s00704-017-2244-0

Gomes, G.F., da Cunha, S.S. and Ancelotti, A.C. (2019), "A sunflower optimization (SFO) algorithm applied to damage identification on laminated composite plates", *Eng. Comput*., **35**(2), 619-626. https://doi.org/10.1007/s00366-018-0620-8

Guan, Y., Mohammadi, B., Pham, Q.B., Adarsh, S., Balkhair, K.S., Rahman, K.U., Linh, N.T.T. and Tri, D.Q. (2020), "A novel approach for predicting daily pan evaporation in the coastal regions of Iran using support vector regression coupled with krill herd algorithm model", *Theore. Appl. Climatol*., 1-19. https://doi.org/10.1007/s00704-020-03283-4

Guven, A. and Kişi, Ö. (2011), "Daily pan evaporation modeling using linear genetic programming technique", *Irrigation Sci*., **29**(2), 135-145. https://doi.org/10.1007/s00271-010-0225-5

Han, Y., Wu, J., Zhai, B., Pan, Y., Huang, G., Wu, L. and Zeng, W. (2019), "Coupling a bat algorithm with xgboost to estimate reference evapotranspiration in the arid and semiarid regions of china", *Adv. Meteorol*., 2019. https://doi.org/10.1155/2019/9575782

Keskin, M.E. and Terzi, Ö. (2006), "Artificial neural network models of daily pan evaporation", *J. Hydrol. Eng*., **11**(1), 65-70. https://doi.org/10.1061/(ASCE)1084-0699(2006)11:1(65)

Khosravi, K., Daggupati, P., Alami, M.T., Awadh, S.M., Ghareb, M.I., Panahi, M., Pham, B.T., Rezaie, F., Qi, C. and Yaseen, Z.M. (2019), "Meteorological data mining and hybrid data-intelligence models for reference evaporation simulation: A case study in Iraq", *Comput. Electron. Agricul*., **167**, 105041. https://doi.org/10.1016/j.compag.2019.105041

Kişi, Ö. (2006), "Daily pan evaporation modelling using a neuro-fuzzy computing technique", *J. Hydrol*., **329**(3-4), 636-646. https://doi.org/10.1016/j.jhydrol.2006.03.015

Luat, N.V., Shin, J. and Lee, K. (2020), "Hybrid BART-based models optimized by nature-inspired metaheuristics to predict ultimate axial capacity of CCFST columns", *Eng. Comput*., **38**, 1421-1450. https://doi.org/10.1007/s00366-020-01115-7

Majhi, B. and Naidu, D. (2021), "Pan evaporation modeling in different agroclimatic zones using functional link artificial neural network", *Inform. Process. Agricul*., **8**(1), 134-147. https://doi.org/10.1016/j.inpa.2020.02.007

Malik, A., Kumar, A., Kim, S., Kashani, M.H., Karimi, V., Sharafati, A., Ghorbani, M.A., Al-Ansari, N., Salih, S.Q., Yaseen, Z.M. and Chau, K.W. (2020), "Modeling monthly pan evaporation process over the Indian central Himalayas: application of multiple learning artificial intelligence model", *Eng. Applicat. Computat. Fluid Mech*., **14**(1), 323-338. https://doi.org/10.1080/19942060.2020.1715845

Mehrabi, M. (2021), "Landslide susceptibility zonation using statistical and machine learning approaches in Northern Lecco, Italy", *Natural Hazards*, **111**(1), 901-937. https://doi.org/10.1007/s11069-021-05083-z

Mehrabi, M. and Moayedi, H. (2021), "Landslide susceptibility mapping using artificial neural network tuned by metaheuristic

algorithms", *Environ. Earth Sci.*, **80**(24), 1-20. https://doi.org/10.1007/s12665-021-10098-7

Mehrabi, M., Pradhan, B., Moayedi, H. and Alamri, A. (2020), "Optimizing an adaptive neuro-fuzzy inference system for spatial prediction of landslide susceptibility using four state-of-the-art metaheuristic techniques", *Sensors*, **20**(6), 1723. https://doi.org/10.3390/s20061723

Moayedi, H., Mehrabi, M., Kalantar, B., Mu'azu, M.A., Rashid, A.S., Foong, L.K. and Nguyen, H. (2019a), "Novel hybrids of adaptive neuro-fuzzy inference system (ANFIS) with several metaheuristic algorithms for spatial susceptibility assessment of seismic-induced landslide", *Geomat. Natural Hazards Risk*, **10**(1), 1879-1911. https://doi.org/10.1080/19475705.2019.1650126

Moayedi, H., Mehrabi, M., Mosallanezhad, M., Rashid, A.S.A. and Pradhan, B. (2019b), "Modification of landslide susceptibility mapping using optimized PSO-ANN technique", *Eng. Comput.*, **35**(3), 967-984. https://doi.org/10.1007/s00366-018-0644-0

Moayedi, H., Mehrabi, M., Bui, D.T., Pradhan, B. and Foong, L.K. (2020), "Fuzzy-metaheuristic ensembles for spatial assessment of forest fire susceptibility", *J. Environ. Manage.*, **260**, 109867. https://doi.org/10.1016/j.jenvman.2019.109867

Moayedi, H., Ghareh, S. and Foong, L.K. (2021), "Quick integrative optimizers for minimizing the error of neural computing in pan evaporation modeling", *Engineering with Computers*, **38**(2), 1331-1347. https://doi.org/10.1007/s00366-020-01277-4

Moazenzadeh, R., Mohammadi, B., Shamshirband, S. and Chau, K.W. (2018), "Coupling a firefly algorithm with support vector regression to predict evaporation in northern Iran", *Eng. Applicat. Computat. Fluid Mech.*, **12**(1), 584-597. https://doi.org/10.1080/19942060.2018.1482476

Mohamadi, S., Ehteram, M. and El-Shafie, A. (2020), "Accuracy enhancement for monthly evaporation predicting model utilizing evolutionary machine learning methods", *Int. J. Environ. Sci. Technol.*, **17**(7), 3373-3396. https://doi.org/10.1007/s13762-019-02619-6

Mohammadhassani, M., Nezamabadi-Pour, H., Suhatril, M. and Shariati, M. (2014), "An evolutionary fuzzy modelling approach and comparison of different methods for shear strength prediction of high-strength concrete beams without stirrups", *Smart Struct. Syst.*, *Int. J.*, **14**(5), 785-809. http://doi.org/10.12989/sss.2014.14.5.785

Mohammadhassani, M., Saleh, A., Suhatril, M. and Safa, M. (2015), "Fuzzy modelling approach for shear strength prediction of RC deep beams", *Smart Struct. Syst.*, *Int. J.*, **16**(3), 497-519. https://doi.org/10.12989/sss.2015.16.3.497

Mohammadi, B. and Mehdizadeh, S. (2020), "Modeling daily reference evapotranspiration via a novel approach based on support vector regression coupled with whale optimization algorithm", *Agricul. Water Manage.*, **237**, 106145. https://doi.org/10.1016/j.agwat.2020.106145

Mohammadi, B., Linh, N.T.T., Pham, Q.B., Ahmed, A.N., Vojteková, J., Guan, Y., Abba, S.I. and El-Shafie, A. (2020), "Adaptive neuro-fuzzy inference system coupled with shuffled frog leaping algorithm for predicting river streamflow time series", *Hydrol. Sci. J.*, **65**(10), 1738-1751. https://doi.org/10.1080/02626667.2020.1758703

Moré, J.J. (1978), *Numerical Analysis*, Springer, pp. 105-116. https://doi.org/10.1007/BFb0067700

Mosavi, A., Faghan, Y., Ghamisi, P., Duan, P., Ardabili, S.F., Salwana, E. and Band, S.S. (2020), "Comprehensive review of deep reinforcement learning methods and applications in economics", *Mathematics*, **8**(10), 1640. https://doi.org/10.3390/math8101640

Mosbah, H. and El-Hawary, M.E. (2017), "Optimization of neural network parameters by Stochastic Fractal Search for dynamic state estimation under communication failure", *Electric Power Syst. Res.*, **147**, 288-301. https://doi.org/10.1016/j.epsr.2017.03.002

Naganna, S.R., Deka, P.C., Ghorbani, M.A., Biazar, S.M., Al-Ansari, N. and Yaseen, Z.M. (2019), "Dew point temperature estimation: application of artificial intelligence model integrated with nature-inspired optimization algorithms", *Water*, **11**(4), 742. https://doi.org/10.3390/w11040742

Nehdi, M. and Greenough, T. (2007), "Modeling shear capacity of RC slender beams without stirrups using genetic algorithms", *Smart Struct. Syst.*, *Int. J.*, **3**(1), 51-68. https://doi.org/10.12989/sss.2007.3.1.051

Nehdi, M., El Chabib, H. and Said, A. (2006), "Evaluation of shear capacity of FRP reinforced concrete beams using artificial neural networks", *Smart Struct. Syst.*, *Int. J.*, **2**(1), 81-100. https://doi.org/10.12989/sss.2006.2.1.081

Nguyen, H., Mehrabi, M., Kalantar, B., Moayedi, H. and Abdullahi, M.A.M. (2019), "Potential of hybrid evolutionary approaches for assessment of geo-hazard landslide susceptibility mapping", *Geomat. Natural Hazards Risk*, **10**(1), 1667-1693. https://doi.org/10.1080/19475705.2019.1607782

Nourani, V., Elkiran, G. and Abdullahi, J. (2019), "Multi-station artificial intelligence based ensemble modeling of reference evapotranspiration using pan evaporation measurements", *J. Hydrol.*, **577**, 123958. https://doi.org/10.1016/j.jhydrol.2019.123958

Qais, M.H., Hasanien, H.M. and Alghuwainem, S. (2019), "Identification of electrical parameters for three-diode photovoltaic model using analytical and sunflower optimization algorithm", *Applied Energy*, **250**, 109-117. https://doi.org/10.1016/j.apenergy.2019.05.013

Qasem, S.N., Samadianfard, S., Sadri Nahand, H., Mosavi, A., Shamshirband, S. and Chau, K.W. (2019), "Estimating daily dew point temperature using machine learning algorithms", *Water*, **11**(3), 582. https://doi.org/10.3390/w11030582

Rezaie-Balf, M., Maleki, N., Kim, S., Ashrafian, A., Babaie-Miri, F., Kim, N.W., Chung, I.M. and Alaghmand, S. (2019), "Forecasting daily solar radiation using CEEMDAN decomposition-based MARS model trained by crow search algorithm", *Energies*, **12**(8), 1416. https://doi.org/10.3390/en12081416

Roy, B., Singh, M.P. and Singh, A. (2019), "A novel approach for rainfall-runoff modelling using a biogeography-based optimization technique", *Int. J. River Basin Manage.*, **19**(1), 67-80. https://doi.org/10.1080/15715124.2019.1628035

Salimi, H. (2015), "Stochastic fractal search: a powerful metaheuristic algorithm", *Knowledge-Based Syst.*, **75**, 1-18. https://doi.org/10.1016/j.knosys.2014.07.025

Sebbar, A., Heddam, S. and Djemili, L. (2019), "Predicting daily Pan evaporation (Epan) from Dam reservoirs in the mediterranean regions of Algeria: OPELM vs OSELM", *Environ. Processes*, **6**(1), 309-319. https://doi.org/10.1007/s40710-019-00353-2

Sebbar, A., Heddam, S., Kisi, O., Djemili, L. and Houichi, L. (2020), "Comparison of Evolving Connectionist Systems (ECoS) and Neural Networks for Modelling Daily Pan Evaporation from Algerian Dam Reservoirs", *Water Resour. Algeria-Part I*, 161-179. https://doi.org/10.1007/698_2020_527

Seifi, A. and Soroush, F. (2020), "Pan evaporation estimation and derivation of explicit optimized equations by novel hybrid meta-heuristic ANN based methods in different climates of Iran", *Comput. Electron. Agricul.*, **173**, 105418. https://doi.org/10.1016/j.compag.2020.105418

Seyedashraf, O., Mehrabi, M. and Akhtari, A.A. (2018), "Novel approach for dam break flow modeling using computational intelligence", *J. Hydrol.*, **559**, 1028-1038.

Shabani, S., Samadianfard, S., Sattari, M.T., Mosavi, A., Shamshirband, S., Kmet, T. and Várkonyi-Kóczy, A.R. (2020), "Modeling pan evaporation using Gaussian process regression K-nearest neighbors random forest and Support Vector machines; comparative analysis", *Atmosphere*, **11**(1), 66. https://doi.org/10.3390/atmos11010066

Shahbazi, Y., Delavari, E. and Chenaghlou, M.R. (2014), "Predicting the buckling load of smart multilayer columns using soft computing tools", *Smart Struct. Syst., Int. J.*, **13**(1), 81-98. http://doi.org/10.12989/sss.2013.13.1.081

Shaheen, M.A., Hasanien, H.M., Mekhamer, S.F. and Talaat, H.E. (2019), "Optimal power flow of power systems including distributed generation units using sunflower optimization algorithm", *IEEE Access*, **7**, 109289-109300. https://doi.org/10.1109/ACCESS.2019.2933489

Shiri, J., Zounemat-Kermani, M., Kisi, O. and Mohsenzadeh Karimi, S. (2020), "Comprehensive assessment of 12 soft computing approaches for modelling reference evapotranspiration in humid locations", *Meteorol. Applicat.*, **27**(1), e1841. https://doi.org/10.1002/met.1841

Shirsath, P.B. and Singh, A.K. (2010), "A comparative study of daily pan evaporation estimation using ANN, regression and climate based models", *Water Resour. Manage.*, **24**(8), 1571-1581. https://doi.org/10.1007/s11269-009-9514-2

Singh, A., Mittal, M. and Kumar, A. (2020), "Predictive modeling of pan evaporation using random forest algorithm along with features selection", *Proceedings of the 10th International Conference on Cloud Computing, Data Science & Engineering* (*Confluence*), Noida, India, January, pp. 380-384. https://doi.org/10.1109/Confluence47617.2020.9057856

Tezel, G. and Buyukyildiz, M. (2016), "Monthly evaporation forecasting using artificial neural networks and support vector machines", *Theore. Appl. Climatol.*, **124**(1-2), 69-80. https://doi.org/10.1007/s00704-015-1392-3

Thom, A.S., Thony, J.L. and Vauclin, M. (1981), "On the proper employment of evaporation pans and atmometers in estimating potential transpiration", *Quarterly Journal of the Royal Meteorological Society*, **107**(453), 711-736. https://doi.org/10.1002/qj.49710745316

Tran, T.T., Truong, K.H. and Vo, D.N. (2020), "Stochastic fractal search algorithm for reconfiguration of distribution networks with distributed generations", *Ain Shams Eng. J.*, **11**(2), 389-407. https://doi.org/10.1016/j.asej.2019.08.015

Wang, L., Kisi, O., Zounemat-Kermani, M. and Gan, Y. (2016), "Comparison of six different soft computing methods in modeling evaporation in different climates", *Hydrol. Earth Syst. Sci. Discuss.*, 1-51. https://doi.org/10.5194/hess-2016-247

Wang, L., Kisi, O., Zounemat-Kermani, M. and Li, H. (2017), "Pan evaporation modeling using six different heuristic computing methods in different climates of China", *J. Hydrol.*, **544**, 407-427. https://doi.org/10.1016/j.jhydrol.2016.11.059

Wang, H., Yan, H., Zeng, W., Lei, G., Ao, C. and Zha, Y. (2020), "A novel nonlinear Arps decline model with salp swarm algorithm for predicting pan evaporation in the arid and semi-arid regions of China", *J. Hydrol.*, **582**, 124545. https://doi.org/10.1016/j.jhydrol.2020.124545

Wu, L., Huang, G., Fan, J., Ma, X., Zhou, H. and Zeng, W. (2020), "Hybrid extreme learning machine with meta-heuristic algorithms for monthly pan evaporation prediction", *Comput. Electron. Agricul.*, **168**, 105115. https://doi.org/10.1016/j.compag.2019.105115

Xie, S.J., Lin, H., Chen, Y.F. and Wang, Y.X. (2021), "A new nonlinear empirical strength criterion for rocks under conventional triaxial compression", *J. Central South Univ.*, **28**(5), 1448-1458. https://doi.org/10.1007/s11771-021-4708-8

Yang, F., Moayedi, H. and Mosavi, A. (2021), "Predicting the degree of dissolved oxygen using three types of multi-layer perceptron-based artificial neural networks", *Sustainability*, **13**(17), 9898. https://doi.org/10.3390/su13179898

Yaseen, Z.M., Ghareb, M.I., Ebtehaj, I., Bonakdari, H., Siddique, R., Heddam, S., Yusif, A.A. and Deo, R. (2018), "Rainfall pattern forecasting using novel hybrid intelligent model based ANFIS-FFA", *Water Resour. Manage.*, **32**(1), 105-122. https://doi.org/10.1007/s11269-017-1797-0

Zhang, G., Band, S.S., Ardabili, S., Chau, K.W. and Mosavi, A. (2022), "Integration of neural network and fuzzy logic decision making compared with bilayered neural network in the simulation of daily dew point temperature", *Eng. Applicat. Computat. Fluid Mech.*, **16**(1), 713-723. https://doi.org/10.1080/19942060.2022.2043187

Zhao, Y. and Foong, L.K. (2022), "Predicting Electrical Power Output of Combined Cycle Power Plants Using a Novel Artificial Neural Network Optimized by Electrostatic Discharge Algorithm", *Measurement*, 111405. https://doi.org/10.1016/j.measurement.2022.111405

Zhao, Y. and Wang, Z. (2022), "Subset simulation with adaptable intermediate failure probability for robust reliability analysis: an unsupervised learning-based approach", *Struct. Multidiscipl. Optimiz.*, **65**(6), 1-22. https://doi.org/10.1007/s00158-022-03260-7

Zhao, Y., Zhong, X. and Foong, L.K. (2021), "Predicting the splitting tensile strength of concrete using an equilibrium optimization model", *Steel Compos. Struct., Int. J.*, **39**(1), 81-93. https://doi.org/10.12989/scs.2021.39.1.081

Zhao, Y., Hu, H., Song, C. and Wang, Z. (2022), "Predicting compressive strength of manufactured-sand concrete using conventional and metaheuristic-tuned artificial neural network", *Measurement*, **194**, 110993. https://doi.org/10.1016/j.measurement.2022.110993

Zheng, S., Lyu, Z. and Foong, L.K. (2020), "Early prediction of cooling load in energy-efficient buildings through novel optimizer of shuffled complex evolution", *Eng. Comput.*, **38**(Suppl 1), 105-119. https://doi.org/10.1007/s00366-020-01140-6

Zuo, H., Chen, B., Wang, S., Guo, Y., Zuo, B., Wu, L. and Gao, X. (2016), "Observational study on complementary relationship between pan evaporation and actual evapotranspiration and its variation with pan type", *Agricul. Forest Meteorol.*, **222**, 1-9. https://doi.org/10.1016/j.agrformet.2016.03.002.

CC